JOURNAL OF Applied Polymer SCIENCE

A Qualitative Assessment of Long Chain Branching Content in LLDPE, LDPE and their Blends via Thermorheological Analysis

Abdol Kamal Dordinejad, Seyed Hassan Jafari
School of Chemical Engineering, College of Engineering, University of Tehran, Tehran, Iran
Correspondence to: S. H. Jafari (E-mail: shjafari@ut.ac.ir).

ABSTRACT: Various blend systems having controlled level of long-chain branching were prepared by melt mixing of different amounts (5, 10, 25, 50, 75, and 90 wt %) of low-density polyethylene (LDPE) with a linear low density polyethylene (LLDPE). Analysis of the branching structure in the blends as well as in the neat components was carried out via thermorheological method. For this purpose six methods including time–temperature superposition (TTS), Cole–Cole plot, van Gurp–Palmen curve, phase angle (δ) versus reduced frequency curve, and activation energy as a function of the δ were employed. The results of all these methods (except TTS) indicated a complex thermorheological behavior for the neat LLDPE and LLDPE/LDPE blends. The extent of complexity was intensified by increasing LDPE content of the blends. However, using TTS method, $E_a(\delta)$ and $\delta(\omega)$ curves resulted in simple thermorheological behavior for neat LDPE. The simple thermorheological behavior of LDPE having high content of long-chain branches (LCB) was attributed to small differences in its branch structures. The zero-shear rate viscosities of all samples deviated from the power-law equation of linear PEs which confirmed the presence of LCB in all the systems. This study shows that thermorheological assessment can be used as an alternative powerful rheological tool for analysis of the branching structures in PE blends. © 2013 Wiley Periodicals, Inc. J. Appl. Polym. Sci. 000: 000–000, 2013

KEYWORDS: blends; polyolefins; rheology; viscosity; viscoelasticity

Received 16 December 2012; accepted 15 May 2013; Published online
DOI: 10.1002/app.39560

INTRODUCTION

Thermorheological investigation is one of the most comprehensive methods to draw useful information about molecular structure of polymers such as polyethylenes (PEs) and their blends.[1–33] Basically, a polymer has a simple thermorheological behavior when a master curve based on time–temperature superposition (TTS) principle can be established. Otherwise it has a complex thermorheological behavior.[26,29] Several other methods such as Cole–Cole plot, van Gurp–Palmen curve, phase angle (δ) versus reduced frequency, and activation energy (E_a) as a function of δ can also be utilized for determination of thermorheological behavior.[1,9,26,28,29,34–36] For all these methods it is necessary to measure viscoelastic properties at different temperatures. One way of distinguishing the complex thermorheological behavior from the simple behavior is based on determination of E_a. When E_a shows no dependency on frequency, modulus, and phase angle a master curve can be established by shifting the measured viscoelastic properties at different temperatures. This is an indication of simple thermorheological behavior. Such behavior has been observed for a linear PE.[26,29] On the other hand, a complex thermorheological behavior has been reported for a long-chain branched metallocene linear low density PE (LCB-mLLDPEs) and low density polyethylene (LDPE). For these materials due to dependency of E_a on frequency, modulus, and phase angle establishment of master curve was impossible.[26]

Some specific energy is needed for relaxation of PE chains. Indeed, one can consider E_a as potential energy needed for this relaxation. Since E_a of linear PE is about 27–28 kJ/mol and it does not depend on molecular weight therefore all its chains have the same level of E_a for relaxation (i.e., E_a is constant) hence it shows a simple thermorheological behavior.[28,36] A branched PE with high content of long chain branching shows different relaxation times and activation energies due to simultaneous presence of long-chain branching and linear chains. The branched chains reduce the segmental dynamic and results in increased relaxation times. The linear chains have lower activation energy as compared to the branched chains. This results in a wide spectrum of relaxations which are not constant. Eventually this leads to a complex thermorheological behavior.[26,28]

In literature, the curves of E_a were studied as functions of storage modulus(G') and phase angle (δ), and phase angle as a function of reduced frequency to establish the thermorheological behaviors of branched PEs.[26,28,36] For LCB-PEs, a decrease

in E_a with an increase in storage modulus was reported[26] which was considered as a sign for thermorheological complexity. If E_a versus storage modulus or phase angle curves remain unchanged it is a sign for thermorheological simplicity.[26,28,36]

Another way of studying thermorheological behavior is van Gurp–Palmen method in which changes in phase angle as a function of complex modulus at different temperatures are recorded.[35] A complex thermorheological behavior leads to a temperature-dependent van Gurp–Palmen curve.[26–28,35,37,38] Cole–Cole curve (plotted as G'' versus G' or η'' versus η' at different temperatures) is also used to study thermorheological behavior of branched PEs and PE blends.[1,9,34,36]

Creation of a master curve using TTS principle is based on shift factors. The time-scale shift factor (horizontal shift factor), a_T, which represents the temperature-dependence of the relaxation time, can be obtained using the method proposed by Mavridis and Shroff.[1,17] a_T is expressed by an Arrhenius equation as follows:

$$a_T(T, T_0) = \exp\left(\frac{E_a}{R}\left[\frac{1}{T} - \frac{1}{T_0}\right]\right) \quad (1)$$

where E_a is the horizontal activation energy, R is the universal gas constant, T is the measurement temperature, and T_0 is the reference temperature. Sometimes to obtain a better superposition, one needs a modulus-scale shift factor (vertical shift factor), b_T, expressed as[1,17]:

$$b_T(T, T_0) = \exp\left(\frac{E_V}{R}\left[\frac{1}{T} - \frac{1}{T_0}\right]\right) \quad (2)$$

where E_V is the vertical activation energy.

Recently lots of attentions were focused on the influence of branching (short and long branches) on the rheological and thermorheological properties of PE and its blends. Investigations on PEs show that LCBs have stronger effects on the rheological properties and more rheological temperature dependency as compared to short-chain branches (SCBs). Thermorheological behavior of PEs and their activation energy values depend on their type, content, and structure of branches.[18–29] Usually in PEs with no LCBs, time-scale shift factor is enough to obtain a master curve. However, for PE with LCB an additional modulus-scale shift factor is also needed.[26–29]

The activation energy of linear PEs has the minimum value and increases with increasing SCB and LCBs. The values of 26–28 (kJ/mol) are reported for the activation energy of linear PEs, while slightly higher values (30–34 kJ/mol) are obtained for linear PEs containing SCBs. An increase in LCB content has stronger effects on the activation energy rather than the increase in SCB content. A maximum activation energy of about 65 kJ/mol has been reported for LDPE which has a great amount of LCBs.[18–29] Moreover, the activation energy of PE blends, e.g. LLDPE/LDPE depends on the LDPE content. By increasing the LDPE content the activation energy of the blend converges toward the activation energy of LDPE.[1,2,5]

For LLDPE/LDPE blends, a complex thermorheological behavior at high LDPE contents and a simple one at low LDPE contents have been reported. It is even possible to observe a simple or complex thermorheological behavior for all compositions, which is because the thermorheological behavior depends on LCB contents, structural distribution of SCB and LCBs, molecular weight, and molecular weight distribution.[1–16] The TTS principle failure for neat PEs is because of LCB, whereas for PE blends it is due to LCB or immiscibility.[1,2,19,20]

Table I. Characteristics of LLDPE and LDPE

Polymer	LDPE	LLDPE
Product	Lupolen 3020 D	LL 1001XV
Producer	BASF	ExxonMobil
M_w (g/mol)	300,000	105,400
M_n (g/mol)	37,500	62,000
M_w/M_n	8	1.7
T_m (°C)	114	120
Density (g cm^{-3})	0.926	0.918

The main objective of the current work is to utilize simultaneously six different analytical approaches based on rheological measurements to investigate and define thermorheological behavior of polymeric blend systems. It is to be noted that some of these individual techniques have been used for different systems previously; however, combination of these techniques as a whole is used for the first time here on a particular blend system. In our related previous work,[36] similar type of investigations were performed on two grades of neat m-LLDPE samples in order to define their thermorheological behavior. In the current work, the focus is on some model blend systems based on PE in order to examine the applicability and ability of these techniques in defining thermorheological behavior of the blends and their relation with branching structure.

One of the innovative features of this work is that a simple blending technique was used in order to induce different levels of branching, in a controlled manner, by diluting a LDPE, having high level of long chain branching, with different contents of a LLDPE. Another interesting feature of the work is that one is able to monitor the influence of the induced long chain branching on thermorheological behavior in a systematic manner. Complex thermorheological behaviors with different extents were observed for the samples with different levels of long chain branching.

EXPERIMENTAL SECTION

Materials

LDPE and LLDPE were provided by BASF (Ludwigshafen, Germany) and ExxonMobile Chemical (Houston, USA) with the commercial names of Lupolen 3020D and LL 1001XV. The main characteristics of polymers are presented in Table I.[39,40] The LLDPE and the LDPE were blended in a twin-screw extruder with L/D of 32 at a screw rotation speed of 150 rpm and a feed of 10 kg/h. The barrel temperatures were 200/210/210/210/220/220°C. LLDPE/LDPE blends with blending ratio of 95/5, 90/10, 75/25, 50/50, 25/75, and 10/90 were prepared.

Rheological Measurements

Parallel-plate rheometry was performed to determine the linear viscoelastic properties of LLDPE/LDPE blends as well as the

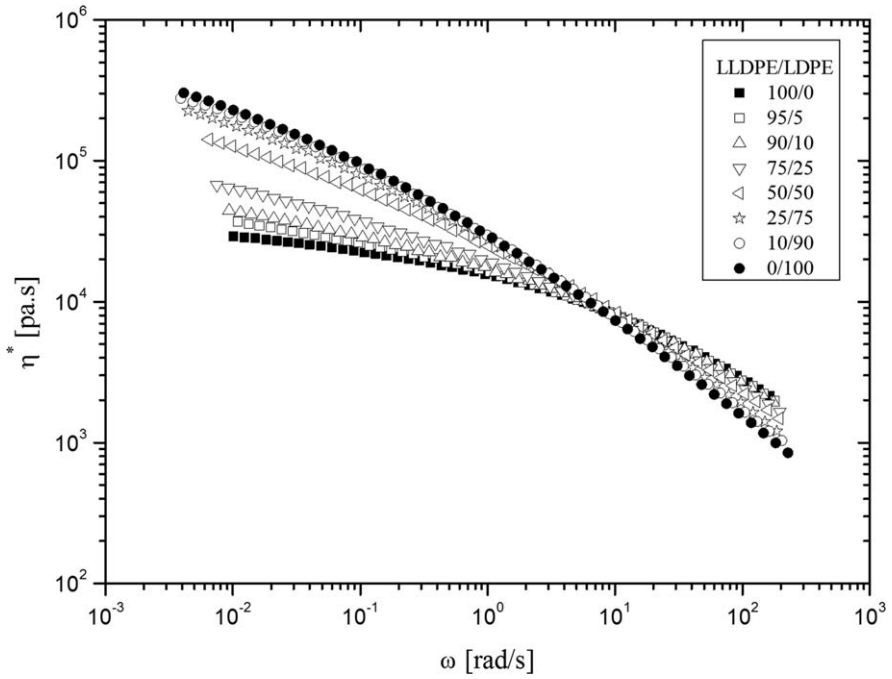

Figure 1. $\eta^*(\omega)$ for blends of LLDPE and LDPE (T_0 = 150°C).

neat components. The measurements were performed using a Paar-Physica Rheometer (MCR300, Ostfildern, Germany) in oscillatory shear mode with parallel plates (25 mm in diameter with a gap of 1 mm) at a wide frequency range from 0.04 to 100 rad/s. The measurements were performed at four different temperatures, i.e. 130, 150, 170, 190, and 210°C with accuracy of ±0.5°C under N_2 atmosphere. All the rheological measurements were performed within linear viscoelastic region.

RESULTS AND DISCUSSION

Rheological Characterization

Figure 1 shows the complex viscosity versus frequency curves of LLDPE/LDPE blends and the neat components. As it is seen from Figure 1, at low frequency, the viscosity of the neat components controls the viscosities of all the blends. Addition of viscous substance (LDPE) to the less viscous component (LLDPE) increases the viscosity of the blend. However, at high frequency, the behavior of the blend is reversed. Additionally, it is observed from Figure 1 that shear thinning for LLDPE occurs at higher frequencies as compared to that for LDPE. Furthermore in the blends, the increase in LDPE content decreases the frequency which signifies the occurrence of shear thinning. This is because of the increase in LCB content with the addition of LDPE.

Stadler et al. obtained the following relationship between zero-shear rate viscosity and weight-average molecular weight for linear PEs at 150°C.[41]

$$\eta_0 = 9\times10^{-15}.M_w^{3.6}. \quad (3)$$

Figure 2 represents the double-logarithmic plot of the zero-shear rate viscosity as a function of the weight-average molecular weight for LLDPE/LDPE blends. As the Newtonian plateau region is not reached for most of the samples, for determination of zero-shear viscosity, Carreau-Yasuda equation can be used[42,43]:

$$|\eta*(\omega)| = \eta_0[1+(\lambda\omega)^a]^{n-1/a} \quad (4)$$

where λ is the characteristic time, "a" the width of the transition and $(n-1)$ is the slope in the shear thinning regime. Also, for determining the weight-average molecular weights of the blends the following equation can be used[44–48]:

$$M_{W\text{blend}} = \sum_i w_i M_{Wi}. \quad (5)$$

For substances containing long branches, the zero-shear viscosity is located above the reference line related to linear PE. Presence of LCB leads to a positive deviation from the reference line.[26] According to the literature, the presence of SCB has slight effect on the zero-shear viscosity.[29] Figure 2 shows a positive deviation from the reference line for LDPE and LLDPE implying the presence of long branches in this polymer. In addition, it can be seen that LDPE has less deviation from the reference line as compared to LLDPE. This is due to high amount of long branches in LDPE which results in a decrease in hydrodynamic radius of LDPE. Even a negative deviation from the reference line is reported in some papers due to the high amount of LCB that is related to statistically branched tree-like molecules.[26,49] As it is seen from Figure 2, LLDPE/LDPE blends at all compositions show positive deviation from the reference line that is mainly due to the presence of long branches.

Figure 3 illustrates the $\eta_0/\eta_0^{\text{lin}}$ as a function of LDPE content where η_0 is the zero-shear viscosity of branched samples (LLDPE/LDPE blends) and η_0^{lin} is the zero-shear viscosity of linear samples with the same molecular weight calculated using

Applied Polymer SCIENCE

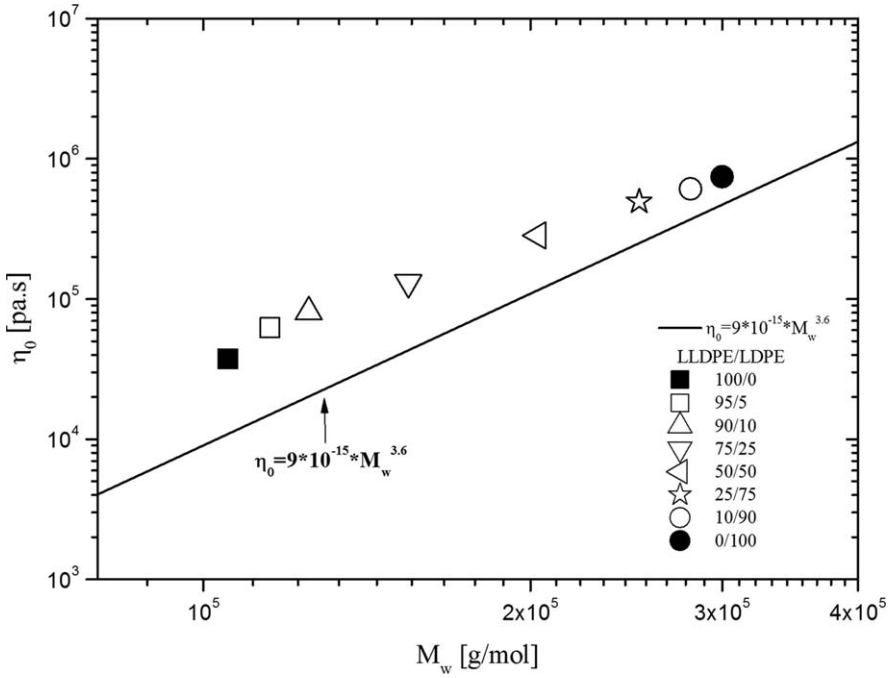

Figure 2. $\eta_0(M_w)$-plot for blends of LLDPE and LDPE (T_0 = 150°C).

eq. (3). As it is seen from Figure 3, only at low LDPE contents $\eta_0/\ \eta_0^{lin}$ increases with LDPE content. By increasing the LDPE content $\eta_0/\ \eta_0^{lin}$ decreases that is due to the reduction of hydrodynamic radius by means of high amounts of long branches.[49]

Time–Temperature Superposition Principle and Determination of E_a

By utilizing TTS principle, one can establish a quantitative evaluation between the thermorheological behaviors of the samples. Obtaining the master curve by shifting G' and G'' (successful application of TTS principle) is usually considered as an indicator of simple thermorheological behavior. Figure 4(a–d) illustrates the double-logarithmic master curves of $b_T G'$ and $b_T G''$ as a function of $a_T\omega$ for the neat components and also for the blends containing 5 and 50% LDPE. A successful application of TTS principle for the neat components and 5% LDPE blend can be observed from Figure 4(a,b,d) which indicates a simple thermorheological behavior. Nevertheless, in Figure 4(c) for 50% LDPE blend, a master curve was not obtained using TTS principle, that can be due to the long branches effect or immiscibility of the blend.[1] The curves obtained for the blends containing 10, 25, 75, and 90% LDPE are similar to Figure 4(c) (not shown here) which indicates complex thermorheological behavior of these blends. Moreover, it should be noted that the maximum deviation was observed in blends with 25, 50, and 75% LDPE contents. One should note that if the vertical shift factor, b_T, is not used, the master curves of Figure 4(a,b,d) cannot be obtained. This leads to complex thermorheological behavior for all samples.

The horizontal and vertical activation energies of samples were determined using the horizontal and vertical shift factors according to eqs. (1) and (2). Values of activation energy are presented in Table II. LLDPE has the minimum value of activation energy which is slightly more than values reported for LLDPEs without LCB, which is due to the presence of long branches. The maximum value is obtained for LDPE that contains large amounts of long branches. The obtained maximum activation energy is in accordance with value reported in literature. An increase in LDPE content of the blends increases the activation energy of the blend. As it is known, the activation energy is independent of molecular weight (M_w) and molecular weight distribution (MWD), therefore the higher activation energy values of blends containing higher LDPE content can be due to the presence of more branches. This increase in activation energy at the high branch content can be attributed to the

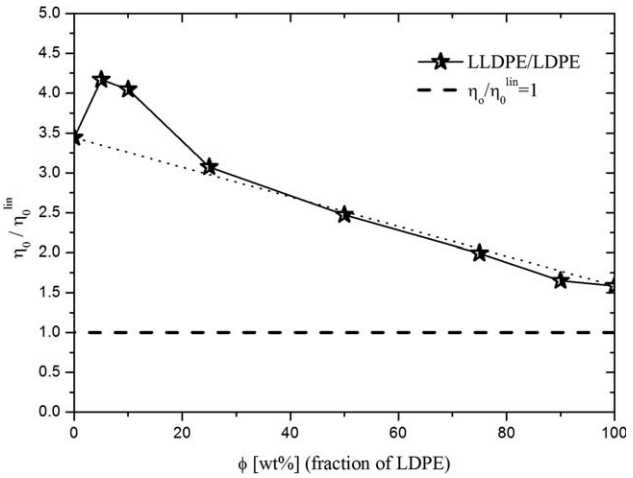

Figure 3. Zero shear-rate viscosity increase factor $\eta_0/\ \eta_0^{lin}$ as a function of weight fraction of LDPE for LLDPE/LDPE blends (T_0 = 150°C).

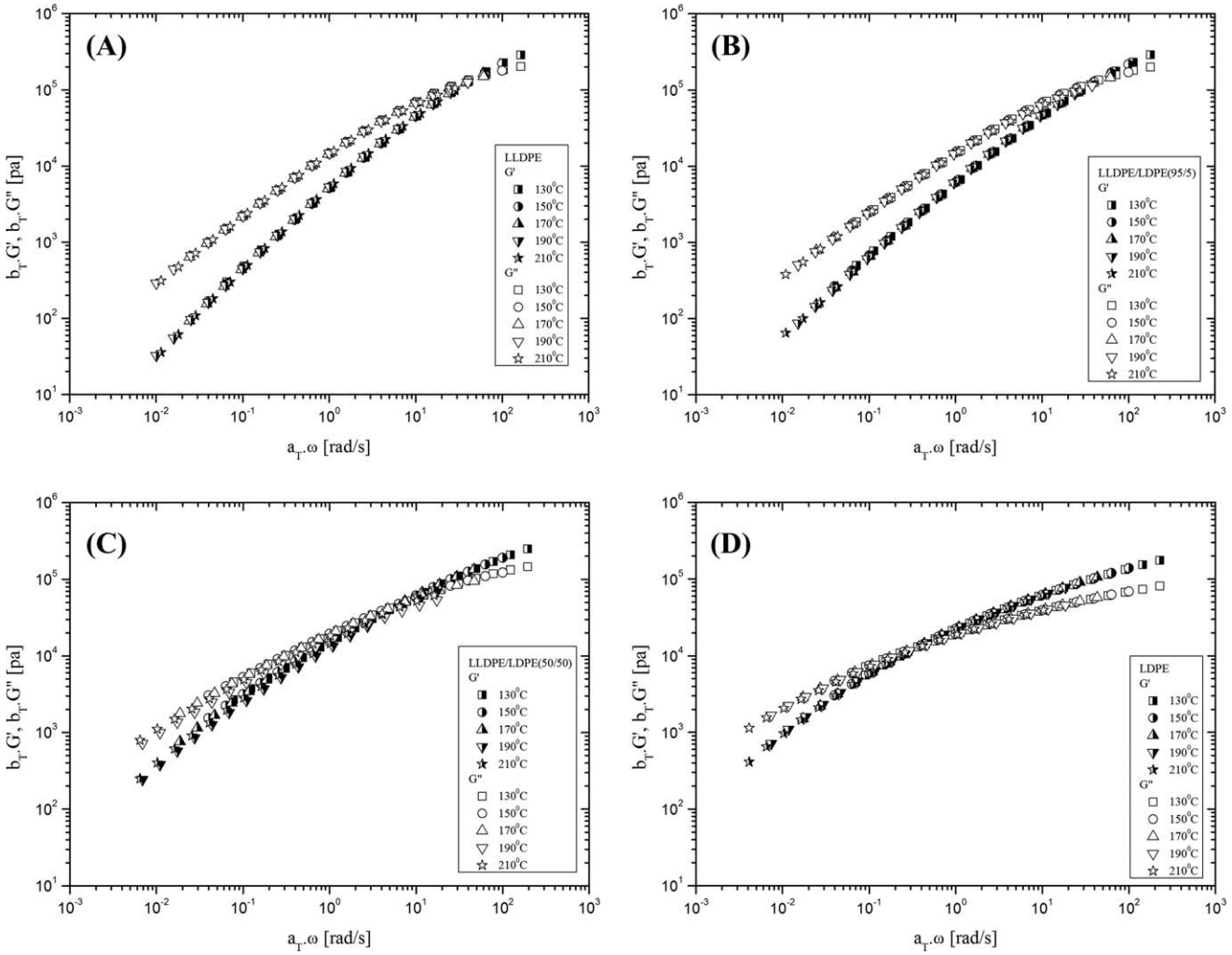

Figure 4. Master curves of the shifted storage modulus ($b_T G'$) and shifted loss modulus ($b_T G''$) as a function of the reduced frequency ($a_T \omega$) for (a) LLDPE, (b) LLDPE/LDPE(95/5), (c) LLDPE/LDPE(50/50), (d) LDPE (T_0 = 150°C).

slowed segmental dynamics.[29] The activation energy is representative of the potential energy from the flow of a molten polymer, therefore introducing LDPE retards the overall dynamics, and consequently higher activation energy is required for the segmental motion.

Figure 5(a,b) shows the horizontal and vertical activation energies as a function of LDPE content. Figure 5(a) indicates that at higher LDPE content, activation energy increases and at 25 and 50% LDPE contents the maximum increase of activation energy is reached. Vertical activation energy of LLDPE/LDPE blends is in the range of 5–13 kJ/mol. Figure 5(b) indicates that the maximum vertical activation energy is obtained for blends with 25, 50, and 75% LDPE contents. According to Figure 5(a,b) it can be deduced that for samples with more complex thermorheological behavior (the blends containing 25, 50, and 75% LDPE), relatively higher increase in E_a and E_V values are observed.

Table II. Activation Energy Values as Concluded by Various Methods

LLDPE/LDPE	100/0	95/5	90/10	75/25	50/50	25/75	10/90	0/100
E_a[a] (kJ/mol)	36	38.4	41.4	48.4	54.8	58.8	62.3	63.8
E_a[b] average (kJ/mol)	34.9	37.6	39.3	45.4	50	54.7	59.2	62
E_a[c] average (kJ/mol)	30.7	31	32.4	35.2	41.8	44.9	50.8	53.8
E_V[a] (kJ/mol)	5	7	8.4	13.1	11.5	11.1	7.5	5.2

[a] E_a and E_V obtained from TTS method.
[b] Average E_a obtained from Kessner and Munstedt method.
[c] Average E_a obtained from Wood-Adams and Costeux method.

Table III. Thermorheological Behavior of LLDPE/LDPE at 150°C as Obtained by Various Criteria

LLDPE/LDPE	100/0	95/5	90/10	75/25	50/50	25/75	10/90	0/100
TTS ($b_T.G'$, $b_T.G''$ versus $a_T.\omega$ plots)	Simple	Simple	C	C	C	C	C	Simple
Cole–Cole (G'' versus G' plots)	C	C	C	C	C	C	C	C
van Gurp-Palmen (δ versus G^* plots)	C	C	C	C	C	C	C	C
δ versus $a_T.\omega$ plots	C	C	C	C	C	C	C	Simple
E_a versus δ plots	C	C	C	C	C	C	C	Simple
E_a versus G' plots	C	C	C	C	C	C	C	C

Simple: thermorheologically simple behavior, C: thermorheologically complex behavior.

Thermorheological Analysis: Cole–Cole Plots

Figure 6 shows Cole–Cole plots (G'' as a function of G') for the neat components and LLDPE/LDPE blends. For better visualization, the curves were shifted along G'' axis using the coefficients shown on Figure 5. For all samples, the Cole–Cole curve does not superpose (note that non-superposition of some samples such as LLDPE is small), which indicates complex thermorheological behavior for all samples. This non-superposition of Cole–Cole plot is related to the presence of long branches in polymer structures.[34]

Thermorheological Analysis Based on van Gurp–Palmen Method

Figure 7 shows the phase angel (δ) plots against complex modulus ($|G^*|$), the so called van Gurp–Palmen plots, at different temperatures for LLDPE/LDPE blends. For better visualization the diagrams were shifted along the G^* axis by multiplying the values with coefficients shown in Figure 7. It is evident that the van Gurp–Palmen plots of LLDPE and LDPE have some maximum and minimum values of phase angle (δ). By increasing the LCB content (increase in LDPE content) of the blends, the diagram shifts to lower values of phase angle which is in good agreement with the literature.[126–28] Non-superposition is observed for both LLDPE and LDPE, which is due to the presence of long branches in both samples. So, it seems this method is more sensitive to the presence of long branches in polymer structure as compared to the TTS principle (superposition in $b_T G'$ and $b_T G''$ against $a_T \omega$ curves).

Furthermore from Figure 7, non-superposition can be observed for all blends. The maximum values of non-superposition are for blends with 25 and 50% LDPE contents. So, based on this method, a complex thermorheological behavior for all the samples is concluded. Also, one should note that there are differences between the thermorheological behavior of LDPE and that of blends. There is a systematic split between the measured data at different temperatures in LDPE diagram, but the shape of the diagram does not change. On the other hand, a split occurs in blends and the diagram shape changes with temperature; however, the systematic split is not observed. In addition, a slight superposition for blends at low-δ (short relaxation time) can be observed, where at higher δ (longer relaxation time) non-superposition and split between the data are observed. This can be attributed to LCB containing molecules with higher relaxation times. The behavior observed for LLDPE/LDPE blends is similar to that reported for LCB metallocene PE.[26,27]

Thermorheological Analysis Based on Phase Angle Curve as a Function of Frequency

Figure 8(a–d) illustrates the phase angle (δ) curve as a function of frequency (ω) for LDPE and the blends containing 10, 25, and 50% LDPE. It is observed from Figure 8(d) that there is no

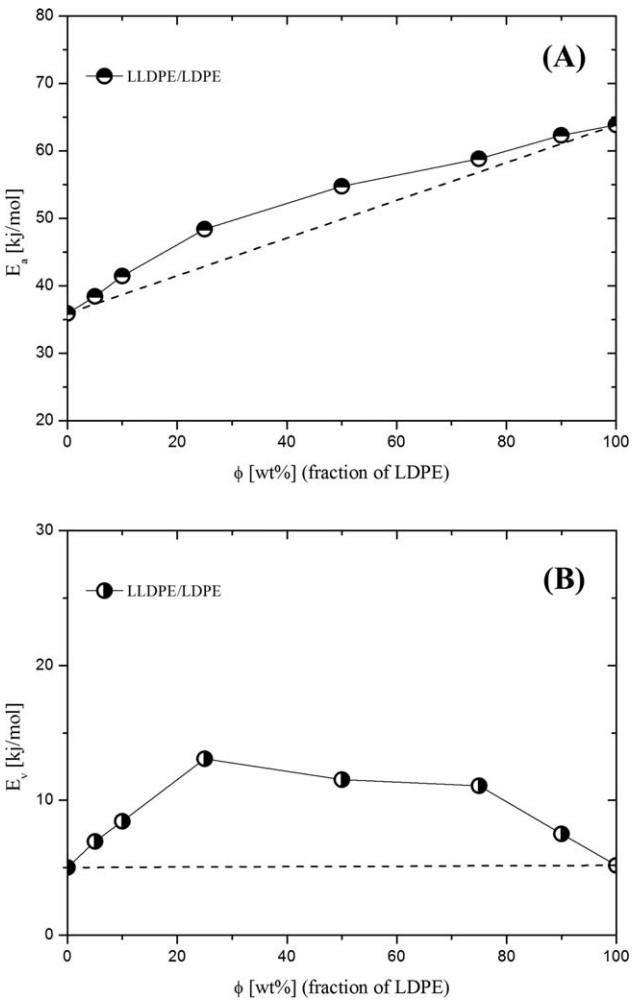

Figure 5. (a) Horizontal activation energy, E_a (kJ/mol), and (b) vertical activation energy, E_v (kJ/mol), as a function of weight fraction of LDPE for LLDPE/LDPE blends.

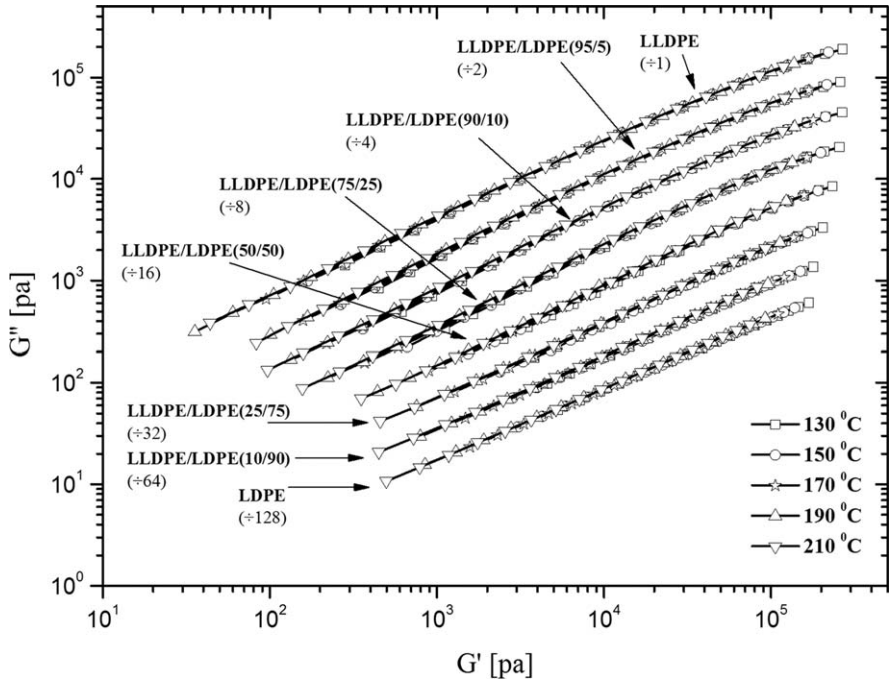

Figure 6. Cole–Cole (G'' vs. G') plots for blends of LLDPE and LDPE (the curves were shifted along the G''-axis by the factors indicated, for the matter of a better visualization).

change in the shape of LDPE curves with temperature, and the curves can be shifted toward each other along the frequency axis to obtain a master curve (Figure 9). However, Figure 8(a–c) shows that the shapes of δ–ω curves change with temperature, which makes it impossible to obtain master curves for these blends.

Figure 9 shows the phase angle of LLDPE/LDPE blends and the neat components as a function of reduced frequency. The curves were shifted along the ω-axis by multiplying the values with the coefficients shown on the diagram for better visualization. Figure 9 indicates that there is a good superposition to obtain a master curve resulting in simple thermorheological behavior for

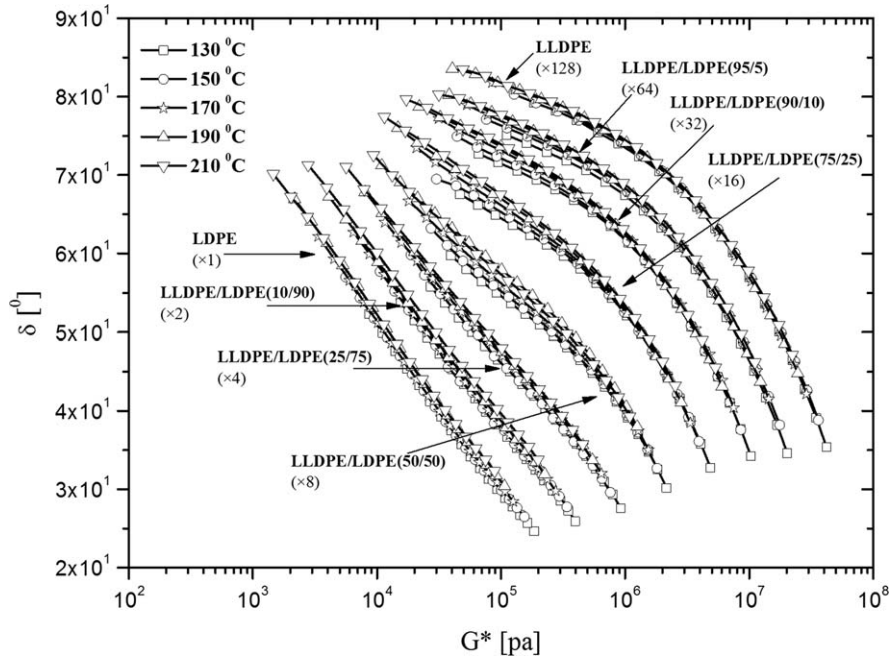

Figure 7. van Gurp–Palmen (δ vs. G^*) plots for LLDPE/LDPE blends (the curves were shifted along the G^*-axis by the factors indicated, for the matter of a better visualization).

Applied Polymer SCIENCE

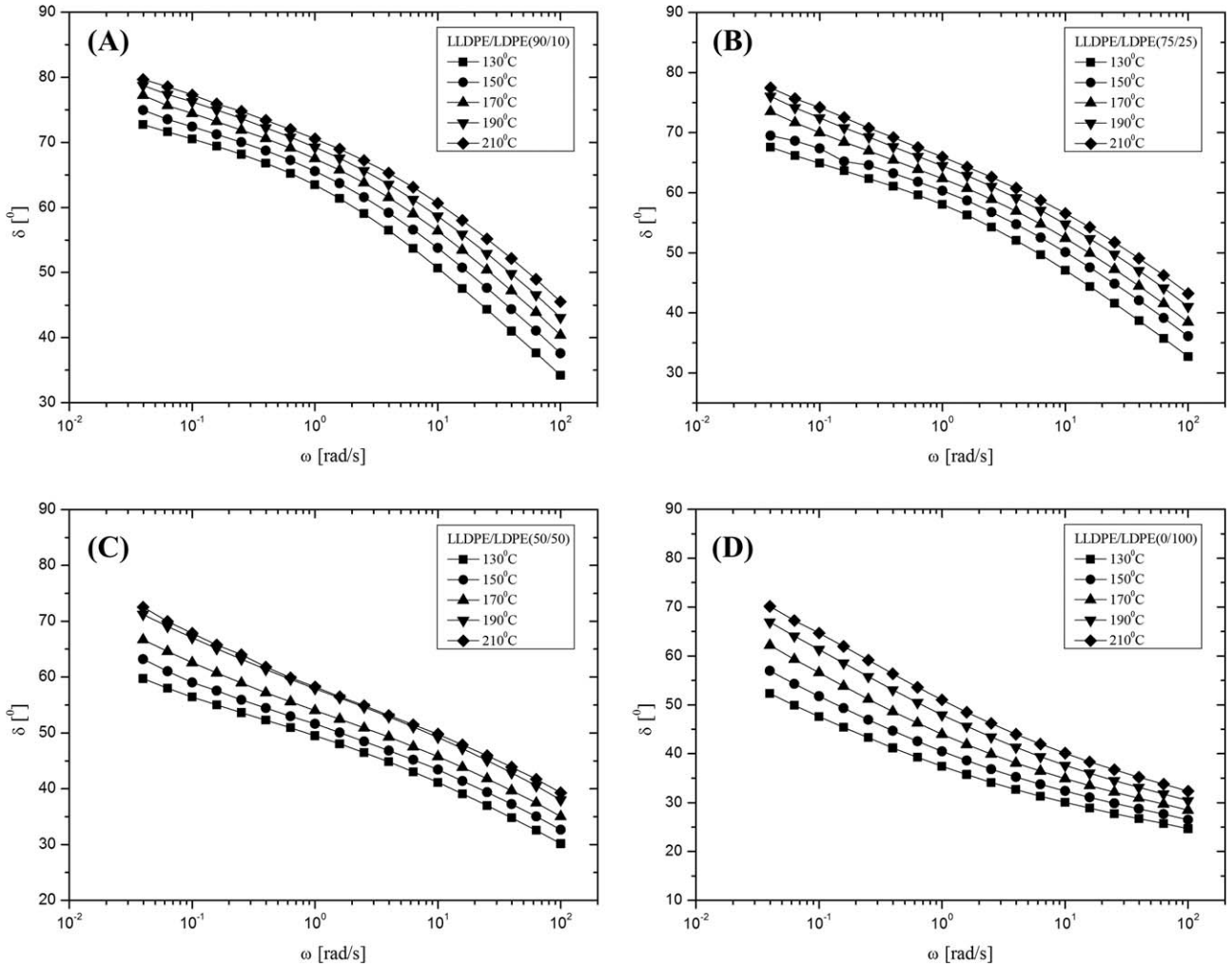

Figure 8. Phase angle δ as a function of the frequency ω at different temperatures for (a) LLDPE/LDPE(90/10), (b) LLDPE/LDPE(75/25), (c) LLDPE/LDPE(50/50), (d) LLDPE/LDPE(0/100).

LDPE. Nevertheless, there is obvious non-superposition for other samples that makes it impossible to obtain a master curve. So based on this method, a complex thermorheological behavior can be concluded for all samples except LDPE.

Thermorheological Analysis: $E_a(\delta)$ According to Kessner and Munstedt Method

To evaluate the thermorheological behavior in greater detail, the activation energy curves as functions of phase angle (δ) can be used. According to Kessner and Munstedt method[26] logarithms of the time-scale shift factors at a constant δ are plotted against the reciprocal absolute temperature $1/T$ [Figure 10(a,b)]. By using Arrhenius relationship for shift factors, the activation energies of LLDPE/LDPE blends and the neat components are plotted as a function of δ in Figure 11. LDPE exhibits constant activation energy. Therefore, based on this method a simple thermorheological behavior is concluded for LDPE. This is similar to the result reported by Kessner et al.[26,28] LLDPE and LLDPE/LDPE blends show phase angle dependent activation energies that indicates complex thermorheological behavior which is attributed to the presence of long branches.[26,28] The

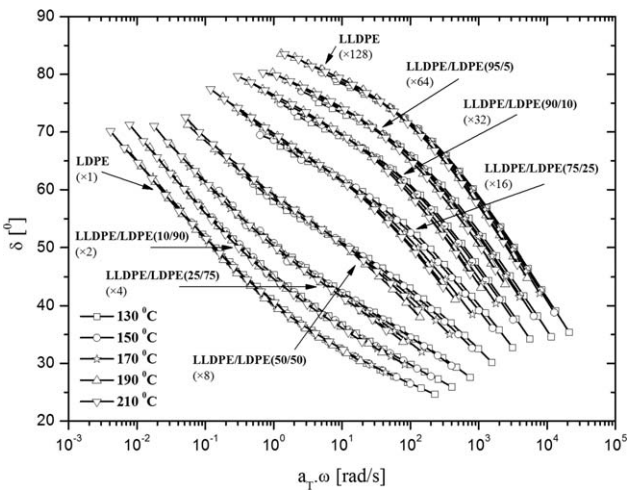

Figure 9. Phase angle δ as a function of the reduced frequency ($a_T.\omega$) at different temperatures for blends of LLDPE and LDPE (the curves were shifted along the ω-axis by the factors indicated, for the matter of a better visualization) (T_0 = 150°C).

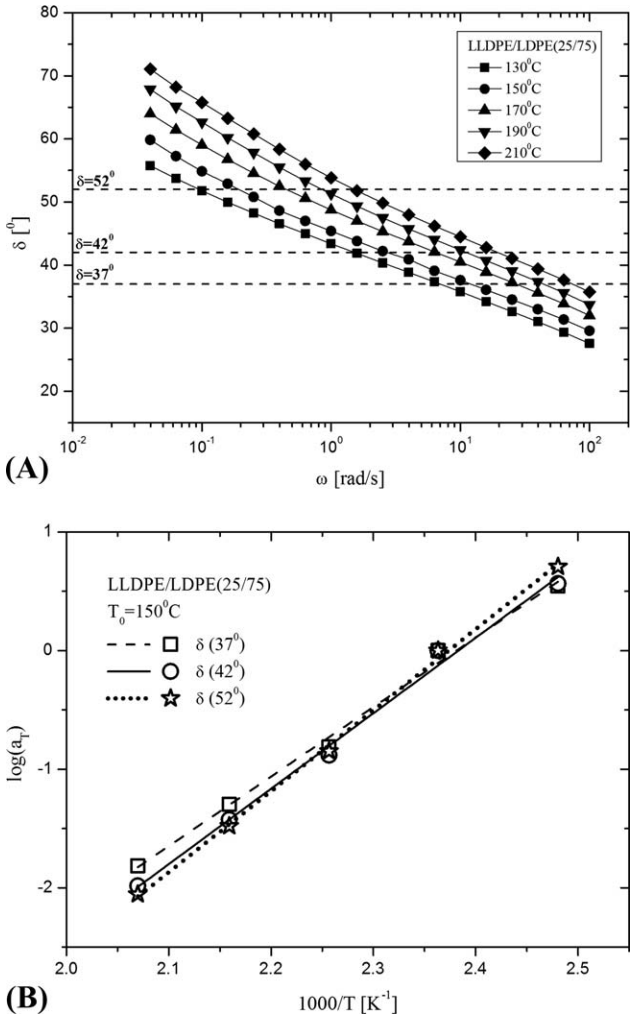

Figure 10. (a) Phase angle δ as a function of the frequency ω at different temperatures for LLDPE/LDPE(25/75) (The dashed lines show the phase angles for which the activation energies were calculated [cf. Figure 10(b)], and (b) Arrhenius-plots of the shift factors for various phase angles of LLDPE/LDPE(25/75) (T_0 = 150°C).

reason for the observed simple thermorheological behavior of LDPE containing high amount of LCB can be the presence of long branches in each LDPE molecule and similarity of the structures of these branches.[27]

$E_a(\delta)$ curve of LLDPE/LDPE blends has three regions. At high δ (longer relaxation time) the activation energy can be considered constant and increases with the increase in LDPE content of the blends. At medium δ values, activation energy is not constant and decreases with the reduction of phase angle. Then again, at third region (low δ) activation energy can be considered constant and has E_a values near the activation energy of linear long-branch-free PEs. This is similar to the behavior reported for LCB-mLLDPEs.[26,28]

Thermorheological Analysis: $E_a(G')$ According to Wood-Adams and Costeux Method

Figure 12 shows the activation energy of LLDPE/LDPE blends as a function of storage modulus according to Wood-Adams and Costeux method.[20] For all samples, dependency of activation energy on the storage modulus was evident. This indicates thermorheological complexity of the samples based on this method. This finding is in agreement with the results reported by Kessner and Munstedt.[26] For all samples, activation energy decreases with the increase in storage modulus. Furthermore, the decreasing rate of the activation energy increases with increase in the long branch content (higher LDPE content).

The average activation energy values for LLDPE/LDPE blends obtained from $E_a(\delta)$ and $E_a(G')$ plots (Figures 11 and 12) are summarized in Table II. These values are plotted along with the activation energy values obtained from TTS as a function of LDPE content in Figure 13. Compared to $E_a(G')$ it is evident that the average activation energy values obtained from $E_a(\delta)$ are closer to those obtained from TTS.

CONCLUSION

The zero-shear rate viscosity showed a deviation from the power-law equation related to the linear PEs in LLDPE/LDPE blends and in the neat components which confirmed the

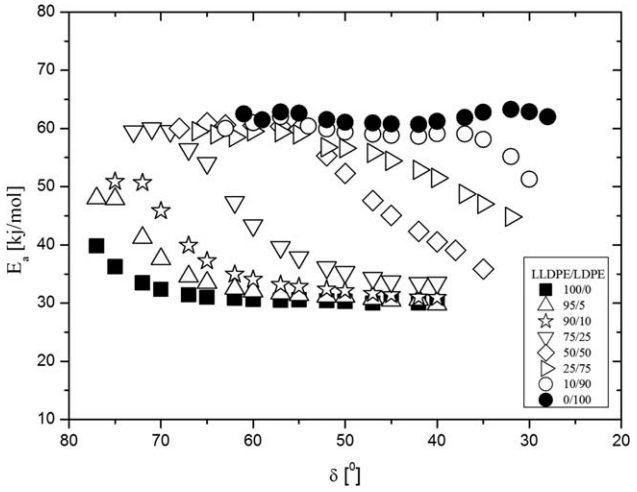

Figure 11. Activation energies, E_a, as a function of the phase angle δ for blends of LLDPE and LDPE.

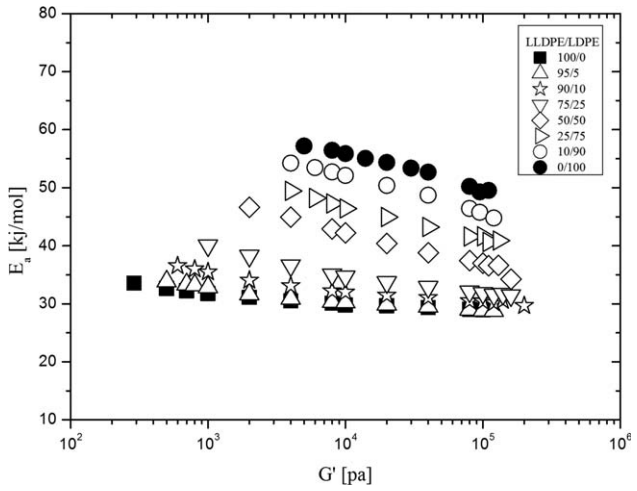

Figure 12. Activation energies, E_a, as a function of the storage modulus G′ for blends of LLDPE and LDPE.

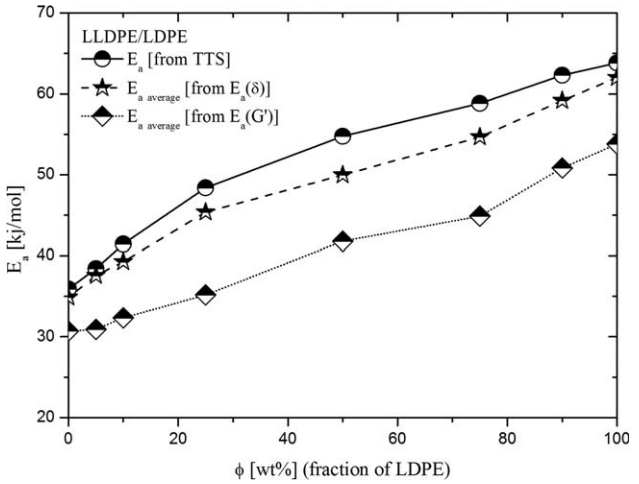

Figure 13. Average activation energies, E_a (kJ/mol), which was obtained from TTS, $E_a(\delta)$, and $E_a(G')$, as a function of weight fraction of LDPE for LLDPE/LDPE blends.

presence of LCB in all the studied samples. Thermorheological behavior of LLDPE/LDPE at various LDPE contents could be determined by employing various analytical approaches. According to the employed different analytical methods (except the TTS), a complex thermorheological behavior was concluded for LLDPE and LLDPE/LDPE blends. However, a simple thermorheological behavior was concluded for LDPE using the approaches based on TTS and $E_a(\delta)$ and $\delta(\omega)$. The simple thermorheological behavior of the LDPE containing high amounts of LCB was attributed to the presence of long branches in each LDPE molecule and similarity of these branch structures. The complexity of thermorheological behavior of blends with low and high LDPE contents was ascribed to the presence of long branches and immiscibility, respectively. Considering the resulting thermorheological behaviors and the horizontal and vertical activation energy values, it was concluded that the most complex thermorheological behavior occurs for the blends containing 25, 50, and 75% LDPE. The calculated activation energy of LLDPE and LDPE being 36 and 63.8 kJ/mol, respectively, were in good agreement with the ones reported in the literature. The activation energy of LLDPE/LDPE blends increases with increase in LDPE contents. Increasing LDPE content (more long-chain branch content) retards the overall dynamics and as a result more activation energy is needed for segmental dynamics. Compared to $E_a(G')$ the average activation energy values obtained from $E_a(\delta)$ were closer to those obtained based on TTS. This study shows that thermorheological assessment can be used as an alternative powerful rheological tool for analyzing the branching structures in PE blends.

The added value of this work is that with the help of simple rheological measurements and by analyzing the data on the basis of combination of six different methods one can gain significant information about branching content, even though it is qualitative. This is just the first step in analyzing the degree of long chain branching by means of thermorheological approach. Using samples with exact structural information would definitely pave the way for establishing a concrete correlation between rheology, thermorheology, and degree of branching in a quantitative manner.

REFERENCES

1. Delgadillo-Velazquez, O.; Hatzikiriakos, S. G.; Sentmanat, M. *Rheol. Acta* **2008**, *47*, 19.
2. Delgadillo-Velazquez, O.; Hatzikiriakos, S. G.; Sentmanat, M. J. *Polym. Sci. Part B: Polym. Phys.* **2008**, *46*, 1669.
3. Liu, C.; Wang, J.; He, J. *Polymer* **2002**, *43*, 3811.
4. Hussein, I. A.; Williams, M. C. *Polym. Eng. Sci.* **2004**, *44*, 660.
5. Yamaguchi, M.; Abe, S. J. *Appl. Polym. Sci.* **1999**, *74*, 3153.
6. Mieda, N.; Yamaguchi, M. *Adv. Polym. Technol.* **2007**, *26*, 173.
7. Cho, K.; Lee, B. H.; Hwang, K. M.; Lee, H.; Choe, S. *Polym. Eng. Sci.* **1998**, *38*, 1969.
8. Hussein, I. A.; Williams, M. C. *Rheol. Acta* **2004**, *43*, 602.
9. Ho, K.; Kale, L.; Montgomery, S. J. *Appl. Polym. Sci.* **2002**, *85*, 1408.
10. Fang, Y.; Carreau, P. J.; Lafleur, P. G. *Polym. Eng. Sci.* **2005**, *45*, 1254.
11. Hameed, T.; Hussein, I. A. *Polymer* **2002**, *43*, 6911.
12. Wagner, M. H.; Kheirandish, S.; Yamaguchi, M. *Rheol. Acta* **2004**, *44*, 198.
13. Gabriel, C.; Munstedt, H. J. *Rheol.* **2003**, *47*, 619.
14. Gabriel, C.; Lilge, D. *Rheol. Acta* **2006**, *45*, 995.
15. Lee, H. S.; Denn, M. M. *Polym. Eng. Sci.* **2000**, *40*, 1132.
16. Hussein, I. A.; Hameed, T.; Sharkh, B. F. A.; Khaled, M. *Polymer* **2003**, *44*, 4665.
17. Mavridis, H.; Shroff, R. N. *Polym. Eng. Sci.* **1992**, *32*, 1778.
18. Vega, J. F.; Santamaria, A.; Munoz-Escalona, A.; Lafuente, P. *Macromolecules* **1998**, *31*, 3639.
19. Malmberg, A.; Liimatta, J.; Lehtinen, A.; Lofgren, B. *Macromolecules* **1999**, *32*, 6687.
20. Wood-Adams, P. M.; Costeux, S. *Macromolecules* **2001**, *34*, 6281.
21. Laun, H. M. *Prog. Colloid Polym. Sci.* **1987**, *75*, 111.
22. Bonchev, D.; Dekmezian, A. H.; Markel, E.; Faldi, A. J. *Appl. Polym. Sci.* **2003**, *90*, 2648.
23. Lohse, D. J.; Milner, S. T.; Fetters, L. J.; Xenidou, M.; Hadjichristidis, N.; Roovers, J.; Mendelson, R. A.; Garcia-Franco, C. A.; Lyon, M. K. *Macromolecules* **2002**, *35*, 3066.
24. Carella, J. M.; Graessley, W. W.; Fetters, L. J. *Macromolecules* **1984**, *17*, 2775.
25. Kokko, E.; Malmberg, A.; Lehmus, P.; Lofgren, B.; Seppala, J. V. J. *Polym. Sci. Part A: Polym. Chem.* **2000**, *38*, 376.
26. Kessner, U.; Munstedt, H. *Polymer* **2010**, *51*, 507.
27. Stadler, F. J.; Kaschta, J.; Munstedt, H. *Macromolecules* **2008**, *41*, 1328.
28. Kessner, U.; Kaschta, J.; Stadler, F. J.; Le Duff, C. S.; Droogh aag, X.; Munstedt, H. *Macromolecules* **2010**, *43*, 7341.

29. Stadler, F. J.; Gabriel, C.; Munstedt, H. *Macromol. Chem. Phys* **2007**, *208*, 2449.
30. Stadler, F. J. *Rheol. Acta* **2012**, *51*, 821.
31. Wang, L.; Yang, B.; Yin, B.; Sun, N.; Feng, J. M.; Yang, M. B. J. *Macromol. Sci. Part B: Phys.* DOI: 10.1080/00222348.2012.660094.
32. Kessner, U.; Kaschta, J.; Munstedt, H. J. *Rheol.* **2009**, *53*, 1001.
33. Mohammadi, M.; Yousefi, A. A.; Ehsani, M. J. *Polym. Res.* **2012**, *19*, 1.
34. Hatzikiriakos, S. G. *Polym. Eng. Sci.* **2000**, *40*, 2279.
35. van Gurp, M.; Palmen, J. *Rheol. Bull.* **1998**, *67*, 5.
36. Dordinejad, A. K.; Jafari, S. H.; Khonakdar, H. A.; Wagenknecht, U.; Heinrich, G. J. *Appl. Polym. Sci.* **2013**, *129*, 458.
37. Stange, J.; Wachter, S.; Kaspar, H.; Munstedt, H. *Macromolecules* **2007**, *40*, 2409.
38. Stadler, F. J. 'Molecular Structure and Rheological Properties of Linear and Long-Chain Branched Ethene-/a-Olefin Copolymers; Sierke-Verlag: Göttingen, **2007**. ISBN 978-3-940333-24-7.
39. Rasmussen, H. K.; Yu, K. *Rheol. Acta* **2008**, *47*, 149.
40. Stary, Z.; Munstedt, H. J. *Polym. Sci. Part B: Polym. Phys.* **2008**, *46*, 16.
41. Stadler, F. J.; Piel, C.; Kaschta, J.; Rulhoff, S.; Kaminsky, W.; Munstedt, H. *Rheol. Acta.* **2006**, *45*, 755.
42. Carreau, P. J. *Trans. Soc. Rheol.* **1972**, *16*, 99.
43. Yasuda, K.; Armstrong, R. C.; Cohen, R. E. *Rheol. Acta.* **1981**, *20*, 163.
44. Friedman, E. M.; Porter, R. S. *Trans. Soc. Rheol.* **1975**, *19*, 493.
45. Montfort, J. P.; Marin, G.; Arman, J.; Monge, P. *Polymer* **1978**, *19*, 277.
46. Bersted, B. H. J. *Appl. Polym. Sci.* **1986**, *31*, 2061.
47. Zang, Y. H.; Muller, R.; Froelich, D. *Polymer* **1987**, *28*, 1577.
48. Peon, J.; Dominguez, C.; Vega, J. F.; Aroca, M.; Martinez-Salazar, J. J. *Mater. Sci.* **2003**, *38*, 4757.
49. Gabriel, C.; Munstedt, H. *Rheol. Acta* **2002**, *41*, 232.